Chapter 6

Influence of micropatterning on the alignment and differentiation of primary myoblasts

6.1. Introduction

Studies on myogenesis are essential considering the need to explore the scientific basis and in-depth understanding of the myogenesis, which may also lead to crucial developments in various myopathies like Duchene muscular dystrophy, Emery-Dreifuss muscular dystrophy and Becker muscular dystrophy (Chal and Pourquié 2017; Folker and Baylies 2013; Rochlin et al. 2010). The anatomy and positioning of the muscle fibres govern the functionality of the skeletal muscle tissue, and muscle cell alignment appears as a prerequisite for myotube formation; emphasizing its role in myogenesis (A. Cooper et al. 2010). Thus, the extent of muscle cell differentiation and their degree of alignment in the tissue model have become critical evaluating criteria for in vitro skeletal muscle models. Amongst all the in vitro methods used for understanding myogenesis, micropatterning is considered as a useful tool as it recreates in vivo like cellular microenvironment (Thery 2010). Substrate micropatterning also helps in understanding the fundamental concepts and mechanisms underlying myogenesis. In early studies, Clark et al. cultured immortalised myogenic cells on laminin micropatterns to explain the mechanism of fusion between myoblasts leading to the formation of linear myotubes. They found that myotubes of constant diameter formed irrespective of the micropattern leading to an idea of lateral fusion prohibition (Clark, Coles, and Peckham 1997). Subsequently, Clark et al. performed another study in microgrooves to demonstrate that fusion in myoblasts occurs in an end-to-end manner and not laterally (Clark et al. 2002). A myriad of micropatterning studies have been carried out to understand its influence on various myogenic properties. The myogenesis properties include myoblast alignment, myoblast fusion, myoblast differentiation, myotubes formation, and acetylcholine receptor sequestration, (Yamamoto et al. 2008; Gingras et al. 2009; N. F. Huang, Lee, and Li 2010; Bajaj et al. 2011; Zatti et al. 2012). Furthermore, several other studies have utilised morphometric based characterisation parameters, e.g., myotube width, fusion

index, and nuclear distribution for assessing differentiation and myotube formation (Agley et al. 2012; Antigny et al. 2013; Bettadapur et al. 2016; Shahini, Choudhury, et al. 2018). In addition, techniques like two-dimensional fast Fourier transform (2D FFT) analysis and orientation order parameter (OOP) have been applied for assessing alignment in muscle tissues (Bajaj et al. 2014; Drew et al. 2015; Feinberg et al. 2012). However, there is a lack of studies relating to the influence of micropatterned contact guidance cues over primary myoblast cell alignment and aligned myotube formation, which leaves room for further intensive research. Relevance for research in the area gains emphasis as studies reports significantly higher levels of adhesion protein expressions in primary satellite cells in comparison to those of C2C12 cells (Grabowska et al. 2011).

In this chapter, primary satellite muscle cells have been studied using morphometric analysis and image processing to reveal their myogenic potential in vitro. For this purpose, an attempt has been made to study the complex and ordered cellular processes that typically result in the acquisition of specific cell fates leading to myogenesis. The primary muscle cells were cultured on micropatterned surfaces having varying widths (20, 200 and 1000 µm) of hydrophilic regimes that were developed by microchannel flowed plasma (µCFP) process using octadecyltrichlorosilane (OTS) and 3-aminopropyltriethoxysilane (APTES) (M.H. Lin et al. 2009). Several characteristic parameters, including the fusion index, maturation index and average width of the myotubes were quantified. Furthermore, nuclear parameters such as area and variation in the number of nuclei concerning a change in myotube width were also analysed. The functional behavior of cultured myotubes exhibiting spontaneous contractions was assessed through kymograph to determine the twitch frequency. 2D FFT based method was used to estimate the extent of myotube alignment in correlation with the alignment of their actin cytoskeleton. These analyses revealed that the µCFP based micropatterned

surfaces not only support differentiation and formation of primary myotubes but also act as a key regulator to control the myotube size. Overall, this study provides a set of morphological and image processing-based methods and identification of specific parameters to characterize the *in vitro* satellite cell myogenesis.

6.2. Materials and method

6.2.1. Materials

Gelatin [Himedia, Mumbai, India], Horse serum [Invitrogen, Bengaluru, India], Pronase [Sigma Aldrich, Bengaluru, India], Hank`s Balanced Salt Solution with (HBSS) [Himedia, Mumbai, India], Dulbecco Modified Eagle`s Medium (DMEM) [Himedia, Mumbai, India], Fetal Bovine Serum (FBS) [Himedia, Mumbai, India], Phosphate Buffered Saline (PBS) [Himedia, Mumbai, India], Paraformaldehyde [Himedia, Mumbai, India], Triton X-100 [Himedia, Mumbai, India], Bovine serum albumin (BSA) [Himedia, Mumbai, India], Poly Vinyl Alcohol 1,4-diazabicyclo[2.2.2]octane (DABCO) [Sigma Aldrich, Bengaluru, India], Poly (dimethyl siloxane) (PDMS) [Dow corning, Michigan, USA], Octadecyltrichlorosilane (OTS) [Sigma Aldrich, Bengaluru, India], 3-Aminopropyltriethoxysilane (APTES) [Sigma Aldrich, Bengaluru, India], n-Hexane [SRL, Mumbai, India], Acetone [SRL, Mumbai, India], PhalloidinTetramethylrhodamine Conjugate[AAT Bioquest, Sunnyvale, California, USA], 4',6-diamidino-2-phenylindole (DAPI) [Himedia, Mumbai, India].

6.2.2. Isolation of satellite cells from rat hind limb skeletal muscle

One-month-old Charles foster rats were sacrificed as per the guidelines of the animal ethical committee of the Institute of Medical Sciences (IMS), Banaras Hindu University (BHU), Varanasi, India. Isolation of cells was performed with minor modifications to the protocol described by Danoviz et al. briefly, lower hind limb muscles tibialis anterior and gastrocnemius were dissected (Danoviz and Yablonka-Reuveni 2012). The muscles were

taken into a Petri plate containing warm Dulbecco`s modified Eagle`s medium (DMEM) with 1% penicillin-streptomycin and washed. Further, muscles were cut into pieces ranging nearly 2-3 mm for facilitating enzymatic digestion in 0.1% pronase in DMEM for 1 h in a CO_2 incubator at 37°C. After enzymatic digestion, the muscle pieces were triturated in a medium consisting of DMEM, 10% horse serum (HS) and 1% penicillin-streptomycin. The triturated cell suspension was plated on a Standard culture grade Petri dish in growth media consisting of DMEM, 20% FBS, 10% HS and 1% penicillin-streptomycin for 1 h under standard CO_2 incubation (Gharaibeh et al. 2008; Jankowski, Deasy, and Huard 2002)**.** The unadhered cells were finally seeded on 2% gelatin-coated culture grade Petri plates at a density of 2.5×10^4 cells /8 cm^2. The growth medium was changed once every 3 days. The cells were further characterised by immunofluorescence staining using antibodies against Pax7 and myogenin at 6 days in vitro.

6.2.3. Micropatterning of hydrophilic and hydrophobic regimes on glass substrates

Glass coverslips were used as substrates to develop repetitive patterns of the monolayers of Octadecyltrichlorosilane (OTS) and 3-Aminopropyltriethoxysilane (APTES). Glass coverslips were oxidised by air plasma (Electro-Technic Product, BD 20AC Laboratory Corona Treater) for 2 minutes on both sides. The oxidised coverslips were immersed in a solution of OTS/n-hexane (1:10000 dilution) for 2 minutes; dried at room temperature to form OTS monolayer on the coverslip. Subsequently, various poly(dimethylsiloxane) (PDMS) stamps with 1000 µm, 200 µm and 20 µm wide stripes with 100 µm height were brought into conformal contact with the OTS-coated coverslips (Figure 6.3) followed by selective oxidation of OTS coated coverslip using PDMS stamps and spring tip electrode of the corona treater for 5 s. The resulting modified glass substrate was next immersed in a solution of APTES/Acetone (1:10000 dilution) for 30 minutes; resulting in repeating patterns of OTS and APTES onto the glass surface (M. H. Lin et al. 2009). Finally, the

micropatterned glass substrates were used for cellular studies by seeding passage number 1 cells at a density of 2.5×10^4 cells/8cm^2. Further, the adherent cells were evaluated for the extent of alignment. Orientation order parameter (OOP) was determined from the bright field images in a time-dependent manner. This parameter has been extensively used in the spatial analysis of liquid crystals and biological structures (Knight et al. 2016; Sheehy et al. 2014); the parameter ranges between 0 for completely unaligned structures and 1 for perfectly aligned structures. For this purpose, we measured angle θ between the direction of the micropatterning and major axis of the cell. OOP was calculated by using the formula OOP= $2[(\cos^2 \theta)-0.5]$ (Umeno and Ueno 2003). The OOP data was obtained from the analysis of at least 10 images from three independent experiments and the data was represented mean±standard deviation.

6.2.4. Bright field and immunofluorescence microscopy

Routine microscopic observations were carried out using bright field images captured with a Nikon TiU microscope. For immunofluorescence microscopy the cells cultured on substrates were fixed with 4% (v/v) paraformaldehyde for 20 minutes at room temperature, permeabilised with 0.1% (v/v) Triton-X 100 detergent for 10 minutes at room temperature and blocked with 1% (w/v) BSA in phosphate buffered saline (PBS) for 30 minutes at room temperature. Further, the cells were incubated with mouse monoclonal primary antibodies of anti-myosin heavy chain primary antibody (MF20) (2.5µg/mL) or anti Pax7 antibody (2.5µg/mL) or anti myogenin antibody (2.5µg/mL) (Developmental Studies Hybridoma Bank (DSHB)) overnight at 4°C followed by incubation with secondary antibody Alexa flour^{TM} 488 goat anti-mouse (1:1000) for 2 hours at room temperature. F-actin and nuclei were stained for 1 hour and 30 minutes, respectively, using PhalloidinTetramethylrhodamine Conjugate (1:1000) and 4',6-diamidino-2-phenylindole (DAPI) (1µg/mL). The cultured glass substrates were further

treated with PVA-DABCO and visualised under the fluorescence microscope. To determine the percentage of Pax7 positive cells a set of 6 images from three different experiments were used to manually count Pax7 positive cells by using Image J (Rueden et al. 2017).

6.2.5. Myotube fusion and maturation indices

Fusion index was estimated by calculating the ratio of the number of nuclei present in the myotube (with at least two or more nuclei) over the total number of nuclei observed. Maturation index was calculated as the percentage of myotube segments having five or more nuclei (Bajaj et al. 2011a). A ratio of number of myotubes having greater than or equal to five nuclei to the total number of myotubes present within a given image was multiplied with hundred to get maturation index in percentage. For the calculation of the indices MHC and DAPI stained fluoroscence images form respective days of 6 DIV, 9 DIV and 14 DIV in culture were used for calculating the indices.The fusion index obtained was further classified into centration fusion index, alignment fusion index and spreading fusion index according to the position of the nuclei within the myotube (W. Roman and Gomes 2018). The index data were obtained from atleast 10 images from three independent experiments, and the data was represented as mean±standard deviation.

6.2.6. Average myotube diameter and nuclear analysis

The captured fluoroscent images were imported in the ImageJ platform. After setting the scale, line region of interest (ROI) tool was used to draw an ROI across the width of the myotube section starting from the top part of the image. Simultaneously, a total of 10 measurements were taken throughout the length of each myotube section, and the average value of the measurements was taken as average myotube diameter.

Using the oval region of interest (ROI) tool, the nucleus present in the image was fitted within the ROI in a manner that should cover the pixels represented by the nucleus to
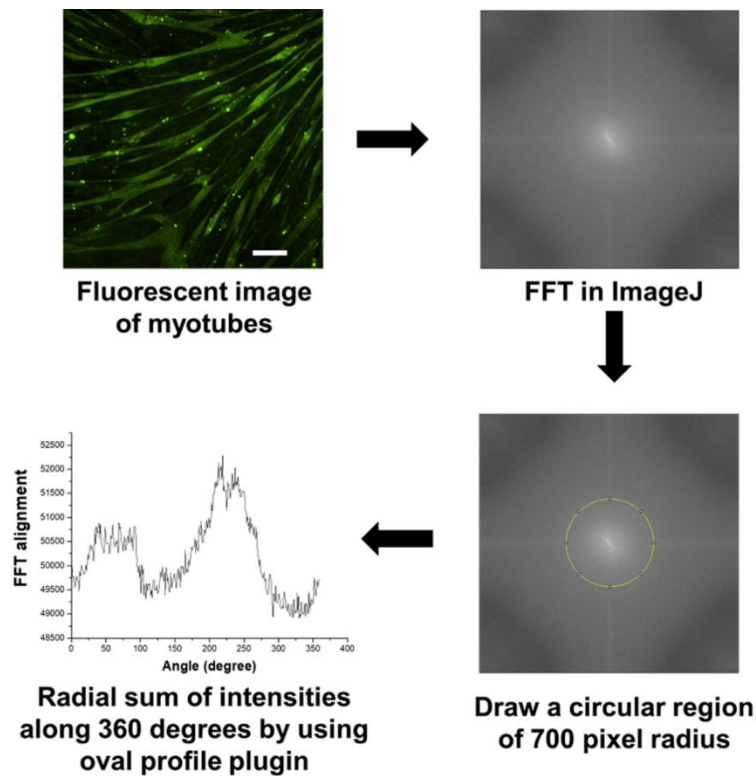
remain inside the ROI. Area measurements of the nuclei were recorded after setting the scale in the software. A mean of measurements from a total of 10 images captured from different regions of the cell culture substrates was calculated. For analyzing the variations in nuclei number with regard to the diameter of myotubes, MHC immunostained fluorescent images of myotubes and nuclei were together imported in the ImageJ platform. The scale was set and a line ROI was drawn across the width of a single myotube containing the nuclei. The number of nuclei present across by the line ROI, i.e., corresponding to the width of myotubes measured was recorded.

6.2.7. Two-dimensional fast Fourier transform (2D FFT) based alignment analysis in myotubes

Myosin heavy chains immunostained images of myotubes cultured on Petri plates and micropatterned glass substrates were used to obtain their respective two-dimensional fast Fourier transform (2D FFT) images. The 2D FFT image represents information pertaining to mathematically defined frequency space domain converted from the corresponding real space domain of the image. This frequency domain can be used to observe the rate of change of pixel intensity distribution present within the image. Using 2D FFT images, further, this rate of change of pixel intensities was plotted around the origin in a manner to represent the degree of alignment within the image. The 2D FFT plot is represented in a way that low-frequency signals and the background signal is placed at the centre, and the high-frequency signals which represent edges and noise are present in the peripheral regions with reference to the origin. A 2D FFT based analysis converts pixel intensities information present in real space of the image into mathematically defined optical data represented in frequency space. Thus, 2D FFT of the image represents a change in pixel intensities throughout the image as a frequency plot. In this study, 2D FFT provided a frequency plot in which cell alignment information around its central pixel is represented in terms of change in grey intensity pixels. Further, these pixel intensities are summed

along the radial direction for each angle of circular projection. These summed intensities plotted against corresponding angle of projection give an FFT alignment plot as shown in Figure 6.1. The pixel intensities of the 2D FFT plot are summed up radially along the circular projection angles by using oval profile plugin (Image J) and plotted against the corresponding angle of acquisition to obtain a 2D FFT alignment plot. Height and overall shape of the peak represent the degree of alignment of myotubes within the image of study. A high and narrow peak represents a uniform degree alignment while a broad peak indicates the presence of more than one axis of alignment of myotubes. For a full random orientation, no recognisable peak will be observed (Bajaj et al. 2011; Ayres et al. 2006).

Fluorescent image of myotubes

FFT in ImageJ

Radial sum of intensities along 360 degrees by using oval profile plugin

Draw a circular region of 700 pixel radius

Figure 6.1 Analysis of myotube alignment using two-dimensional fast Fourier transform. The step-by-step process of analysing the alignment of myotubes using fluorescent images in ImageJ (Scale bar: 100 µm).

6.2.8. Two-dimensional fast Fourier transform (2D FFT) based alignment analysis of actin cytoskeleton in myotubes

Actin filaments immunostained fluorescent images corresponding to the myosin heavy chain images were used to obtain their respective two dimensional fast fourier transform (2D FFT) plots, as shown in Figure 6.1. A Similar procedure, as described for assessing myotube alignment, was employed for determination of actin alignment in relation to the myotube alignment.

6.2.9. Determination of twitch frequency of the spontaneous contraction in myotubes

Time series of images representing the myotube contraction were acquired in a video format using Nikon Ds Qi-2 monochrome camera attached with Nikon Ti-U bright field microscope. A line ROI was drawn at the location of maximum movement on the myotube. Kymograph is a simplified way of representing the dynamics of the twitching process on a single image. A kymograph of the captured video was generated using the kymograph builder plugin in Fiji application, an open source image processing software (Bajaj et al. 2011). The intensity values obtained form the kymograph were normalised by using the formula normalised intensity = (Intensity at a specific time - Intensity minimum)/(Intensity maximum- Intensity minimum). A plot of normalised intensity vs time is plotted. Further, FFT function was applied to the normalised intensity values of the kymograph using OriginLab software, to generate a power versus frequency plot that finally can be used to interpret the level of principal frequency of spontaneous contraction of myotube.

6.2.10. Statistical Analysis:

A set of three experiments were performed and ten images were considered for morphometric analysis from each set of experiment. Statistical analysis was performed by using one way ANOVA post hoc Tukey means of comparison. The data were represented in the form of mean±standard deviation.

6.3. Results and discussion

6.3.1. Dynamics of satellite cells isolated from rat hind limb muscle

Pax7 and myogenin were used to characterize the myogenic nature of the isolated cells as shown in (Figure 6.2A) and (Figure 6.2B) (Shefer, Rauner, Yablonka-Reuveni, & Benayahu, 2010; Wright, Sassoon, & Lin, 1989). Both the cellular markers were traced in culture for 6 days in vitro (DIV) through fluorescence microscopy. About $74\pm3.3\%$ of the cells were stained positive for Pax7, a marker for proliferating myoblasts (Patrick Seale et al. 2000; Hindi et al. 2017).
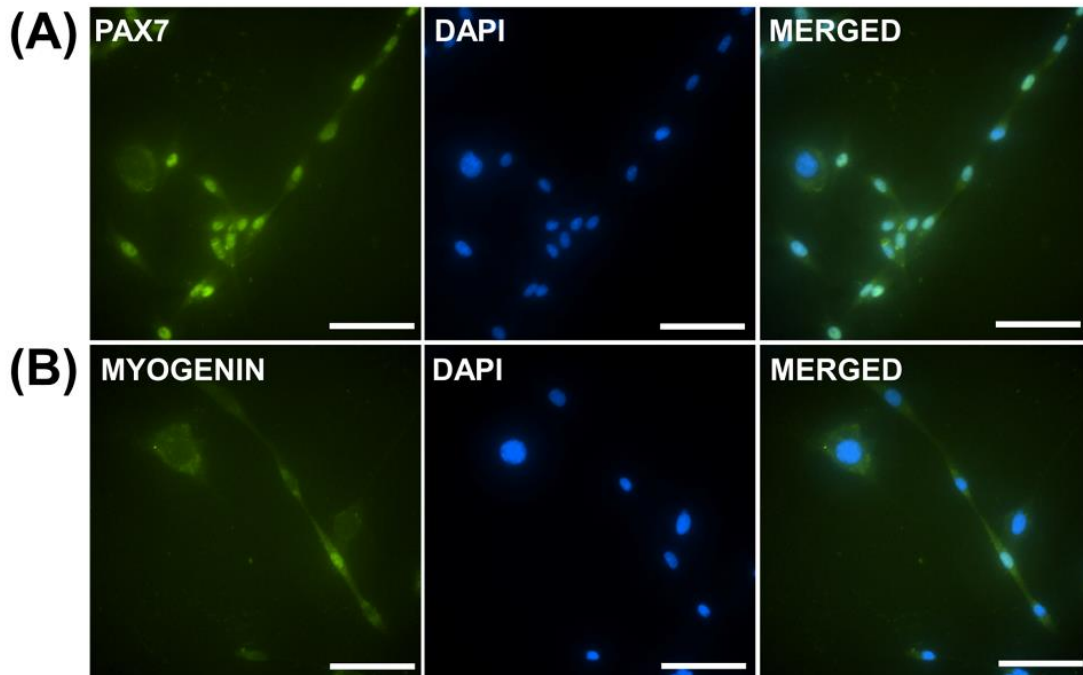
Figure 6.2 depicts merged fluorescence image of isolated myoblasts cultured on 2% gelatin surface stained by using anti PAX7 antibody (green-PAX7 transcription factor) /anti myogenin antibody (green-myogenin myogenic regulatory factor), DAPI (nucleus-blue) respectively. This confirms the presence of proliferating myoblasts.

6.3.2. Micropatterning of satellite cells on glass substrates

To recapitulate in vitro, the aligned pattern of elongated myotubes similar to that of the muscle fibres in vivo, we have utilised a micropatterning technique to create different cell adherent repeating patterns of 1000 µm, 200 µm, and 20 µm widths on glass substrates.

For this purpose, two chemical compounds, i.e., OTS and APTES were exploited to coat the glass surface in a certain order using a Poly (dimethyl siloxane) (PDMS) mould; giving rise to the repeating patterns of hydrophobic and hydrophilic regions, respectively (Figure. 6.3).
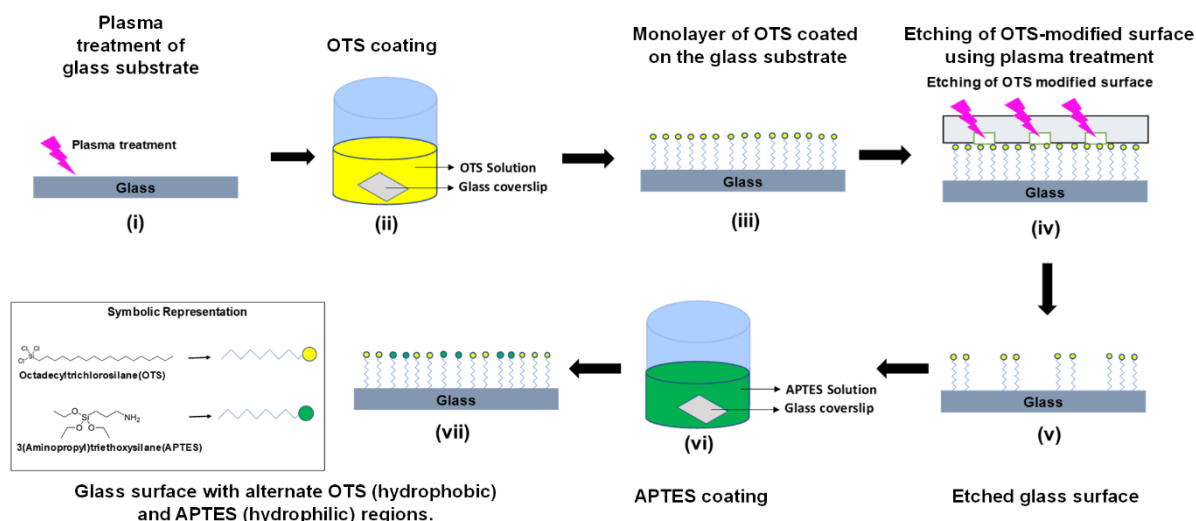

Figure 6.3 Schematic of Microchannnel flowed plasma (µCFP) based micropatterning using OTS (hydrophobic) and APTES (hydrophilic) on glass substrates. (i) Plasma treatment of glass substrate, (ii) OTS coating, (iii) a monolayer of OTS coated on the glass surface, (iv) etching of OTS-modified surface using plasma treatment. (v) etched glass surface (vi) APTES coating (vii) glass surface with alternate OTS (hydrophobic) and APTES (hydrophilic) regions. Analysis of myotube alignment using two-dimensional fast Fourier transform (A) step-by-step process of analysing the alignment of myotubes using fluorescent images in ImageJ (Scale bar: 100 µm).

The procedure adopted in the study is microchannnel flowed plasma (µCFP) for micropatterning surface assembled monolayers of OTS and APTES. The process involves selective exposure of plasma on a self-limiting layer of OTS via PDMS devices to chemically modify the hydrophobic surface, followed by grafting of APTES to create hydrophilic patterns. Using this approach centimetre to nanoscale resolution patterns can be fabricated (M.H. Lin et al. 2009). This ink free soft lithography method overcomes various apprehensions of microcontact printing such as fidelity of pattern transfer, uniformity of large-area processing and possibility of hierarchical structures ranging from nanometres to centimetres. All these concerns are majorly related to transfer of ink

130

between a PDMS stamp and patterning surface placed in conformal contact. Such concerns arise majorly due to stamp deformation and lateral diffusion of ink (M.H. Lin et al. 2009; Sharpe et al. 2005). µCFP eliminates these issues as no external pressure is required for patterning which also reduces the need of weights for applying pressures. Moreover, the replicated patterns show greater fidelity as the mould does not undergo mechanical deformation on repeated usage (M.H. Lin et al. 2009; Lipomi et al. 2012). The micropatterned substrates were plated with satellite muscle cells at passage #1, i.e., satellite cells were cultured on standard culture plates for six days and then re-plated on the micropatterned glass surfaces. Morphological observations indicated that the cells cultured within the widths of 20 µm and 200 µm showed excellent alignment well within the first few days of the culture compared to 1000 µm width as shown in bright-field images (Figure 6.4A, 6.4B, and 6.5A, 6.5B). The cell under micropatterned conditions assumed three morphologies namely polygonal, bipolar, and elongate morphology. These morphological observations are quantified with respect to cell population in each of the micropatterned conditions as shown in Figure 6.6. Figure 6.6A represents the variation in myoblast cell population on 1000 µm patterned substrates over a period of 12 days. By DIV 3 the myoblasts majorly adapted to a bipolar, polygonal morphology along with a few favouring elongated morphologies owing to the stress generated at the peripheral regions of the micropattern. By DIV 6 it was observed that there was a significant increase in polygonal morphology cells compared to the other morphologies owing to the addition of the medium enriched with fresh serum. Further, during DIV 9 the micropatterned environment promotes differentiation of cells due to which bipolar morphology cells are favoured. By DIV 12, increasing fusion events between the differentiated myoblasts lead to a significant increase in elongated morphology of cells throughout the micropatterned surface.
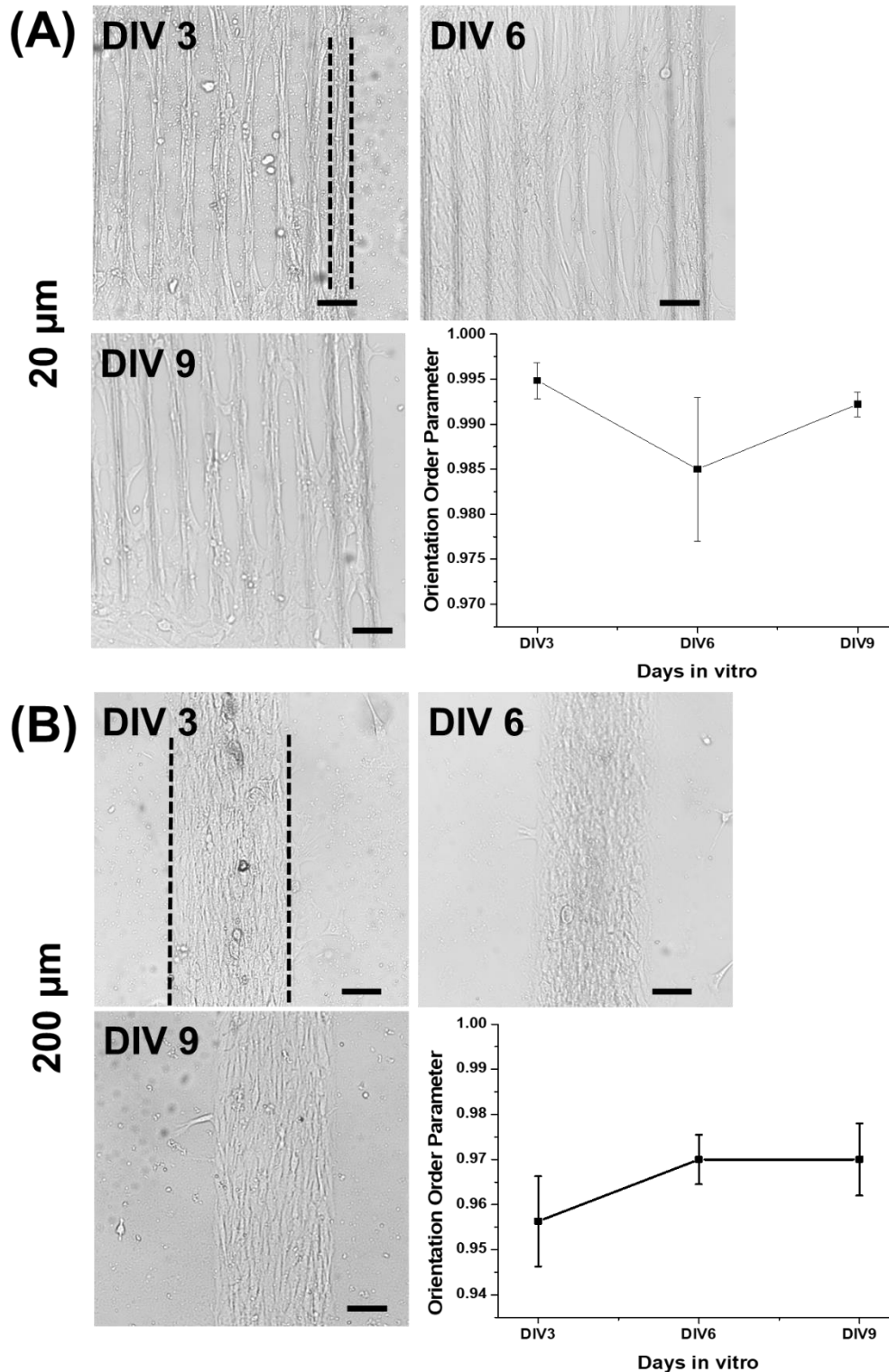
Figure 6.4 Micropatterning of the isolated cells on varying widths and orientation order parameter-based alignment analysis (A) Bright-field images of cells cultured on 20 µm width revealing their aligned morphology at DIV 3, DIV 6 and DIV 9 (Scale bar: 50 µm); a graph showing corresponding orientation order parameter values. (B) Bright-field images of cells cultured on 200 µm width revealing their aligned morphology at DIV 3 and DIV 6 and DIV 9 (Scale bar: 50 µm).
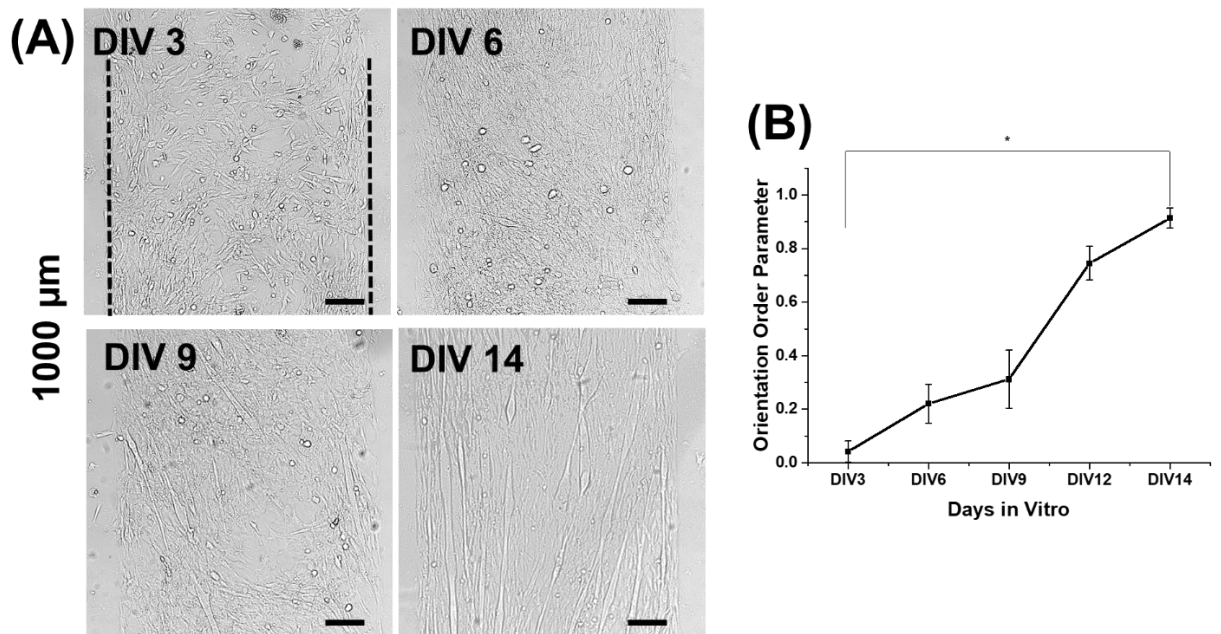
Figure 6.5 Micropatterning of the isolated cells on 1000 µm width and its orientation order parameter-based alignment (A) Bright-field images of cells revealing the various stages of alignment on a micropatterned glass substrate having a 1000 µm width over a period of 14 days (Scale bar: 100 µm); (B) A graph showing corresponding orientation order parameter values. A significant difference was observed between OOP values for 14 DIV and 3 DIV at 0.05 level of significance.

Figure 6.6B represents cell population dynamics when they are cultured on 200 µm micropatterned substrates wherein the myoblasts readily adapt to polygonal and bipolar morphologies along with a few elongated morphology cells by DIV 3. By DIV 6, we observed similar to that of standard and 1000 µm a significant increase in the number of polygonal morphology cells compared to bipolar and elongated morphology due to the addition of fresh medium.

By DIV 9, there was an increase in bipolar morphology due to enhanced differentiation of myoblasts under confined cell adhesion. After 9 DIV, cells got detached from

micropatterns.
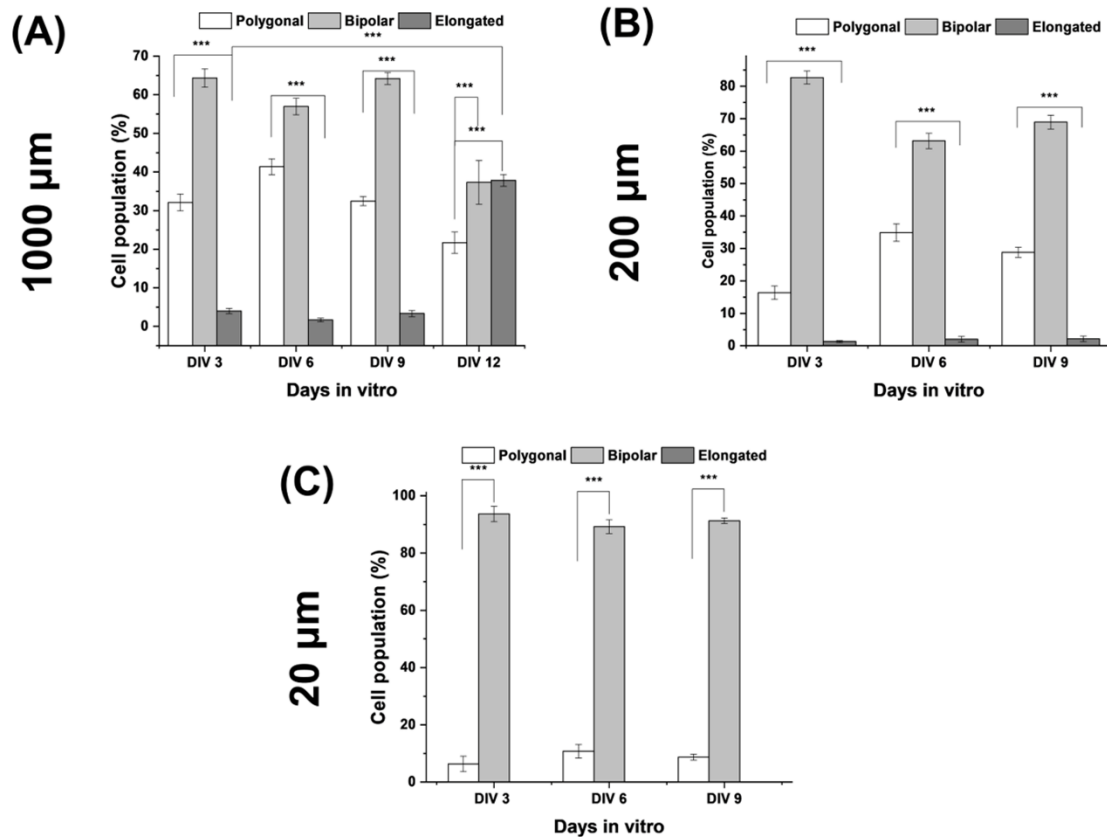
Figure 6.6 Morphology based cell population dynamics of isolated myoblasts on micropatterned surfaces: (A) 1000 µm micropatterns over a period of 12 days, (B) 200 µm micropatterns over a period of 9 days and (C) 20 µm micropatterns over a period of 9 days Significance levels are presented as ***$p<0.001$, **$p<0.01$ and *$p<0.05$.

Similarly, Figure 6.6C represents the cell morphology dynamics for myoblasts cultured on 20 µm micropatterned substrates over a period of 9 days. At DIV 3, the morphology of the cells was bipolar with a few cells having polygonal shape. No cells having elongated morphology were observed during this period. Such an observation may be attributed to the narrow cell adhesive regions of the micropatterns. The cells continued to show similar trends of morphology during DIV 6 and DIV 9. After DIV 9 cell detachment from the micropatterns was observed. No observations of elongated morphology indicate that the micropatterning most likely did not favour fusion between the myoblasts under the given culture condition, which may be attributed to the restricted locomotion of myoblasts within the confined region of micropatterns. Such an observation of inhibited

134

fusion has been reported by clark et al. (Clark et al. 2002). Also, detachment of the muscle cell from micropatterns has been reported by various other groups (Bajaj et al. 2011; S. T. Cooper et al. 2004).

An immediate alignment in case of 20 µm and 200 µm widths was likely to be observed due to the relatively limited surface area available for cellular adhesion compared to those of 1000 µm width. In addition, for the given cell density used for culture, micropatterned substrate possessing 1000 µm hydrophilic regime provided a noticeable window period for the spatiotemporal observation of cellular behaviour. These observations were taken into consideration for the selection of 1000 µm patterned substrates for further evaluation of contact guidance-based alignment of myoblasts. Figure 6.5A shows the bright-field images of the cells cultured on the micropatterned glass surface with a 1000 µm width. By the third day in vitro, the cells with their bipolar morphology adhered to the APTES-coated region. Subsequently, cells after six days in vitro showed the events of fusion to develop a few premyotubes. The micropatterned environment further enhanced the fusion events leading to the formation of short myotubes by 9 days in vitro. Well-elongated myotubes were observed by 14 days in vitro on a micropatterned surface (Figure 6.5A).

### 6.3.3. OOP analysis and contact guidance-based alignment

OOP analysis for the cells cultured on the substrates having patterning widths of 20 µm, 200 µm, and 1000 µm was performed to predict the degree of cellular alignment as shown in Figure 6.4A, Figure 6.4B and Figure 6.5A, respectively. The OOP analysis for 20 µm and 200 µm widths reiterates the immediate alignment of myoblasts within a few days of culture. There was no significant difference observed in the OOP values for 20 µm width from DIV 3 to DIV 9, and the OOP values remained very close to 1 indicating cellular alignment along the micropatterns. A similar conclusion could be drawn from 200 µm width where OOP values for DIV 3 and DIV 9 were found to be 0.96 and 0.97,

respectively. These OOP results further substantiate the early alignment of myoblasts in 20 and 200 µm widths; thus, not allowing the window period for spatiotemporal observation of contact guidance-based alignment of the myoblasts. OOP analysis further revealed that the cells cultured on 1000 µm patterns exhibited an increase in alignment with time to attain an OOP value of 0.93 by DIV 14. A significant difference in the OOP values between DIV 3 and DIV 14 can be seen in this case. This increase in cellular alignment over time could be attributed to the phenomenon of contact guidance as reported in various micropatterning scenarios. Findings indicate that the phenomenon of contact guidance drives the cell to elongate along the grooves or ridge axes (Cimetta et al. 2009; Yamamoto et al. 2008; Zatti et al. 2012). As illustrated from the morphological observation of cells cultured on a micropatterned surface (Figure 6.5A), cells lying closer to or at the interface of hydrophilic and hydrophobic regions were the foremost to get aligned parallel to the micropatterned regimes, while cells adhered farther away from the interface of hydrophilic and hydrophobic regions displayed irregular morphology and random arrangements. However, the entire population of the cells in due course of time manifested a remarkable level of rearrangement and overall alignment. Such observations indicate that cells located at the junction of hydrophilic and hydrophobic regions are likely to be influenced by the surface and cell cues. The cells present at the intersection region may experience non-uniform forces due to spatial anisotropy and thereby result in a cellular alignment that possibly serves further as a cell cue for the adjacent cells to direct them in similar cohorts (Bajaj et al. 2011a; Nava, Raimondi, and Pietrabissa 2014; Zatti et al. 2012). In addition, a study by Junkin et al. supports a similar mechanism of cellular alignment wherein under micropatterned conditions differentiating myoblasts were observed self-organised by communication of orientation information over long range distances (~1000 µm) leading to overall alignment. The self-organisation of

differentiating myoblasts was attributed to the autocatalytic alignment feedback (Junkin, Leung, Whitman, et al. 2011). OOP based on cell morphology has been analysed in a varied number of cells like smooth muscle cells (Umeno et al. 2001; Umeno and Ueno 2003), fibroblasts (Sun, Tang, and Ding 2009), vascular endothelial cells (Palmer and Bizios 1997); major axis of these cells made an angle with respect to director of the alignment. The aligned cells in all the cases showed OOP values close to 1 in the presence of director. Similarly, in the current work, we analysed the OOP for myoblasts under the influence of micropatterned contact guidance cues and obtained an OOP value closer to 1 over a period of 14 days in culture.

6.3.4. Quantification of fusion and maturation indices

The differentiated myoblasts undergo fusion by exiting the cell cycle and form into myotubes. Characterisation of the myotubes is essential to explore the potential of differentiation capability of the isolated cells (Bader, Masaki, and Fischman 1982). Figure 6.7 shows representative fluorescence images of the myotube stained with myosin heavy chain (green) and nuclei (blue) for the isolated cells cultured for 14 days in a standard Petri plate (upper panel) and on a micropatterned glass surface (lower panel), respectively.
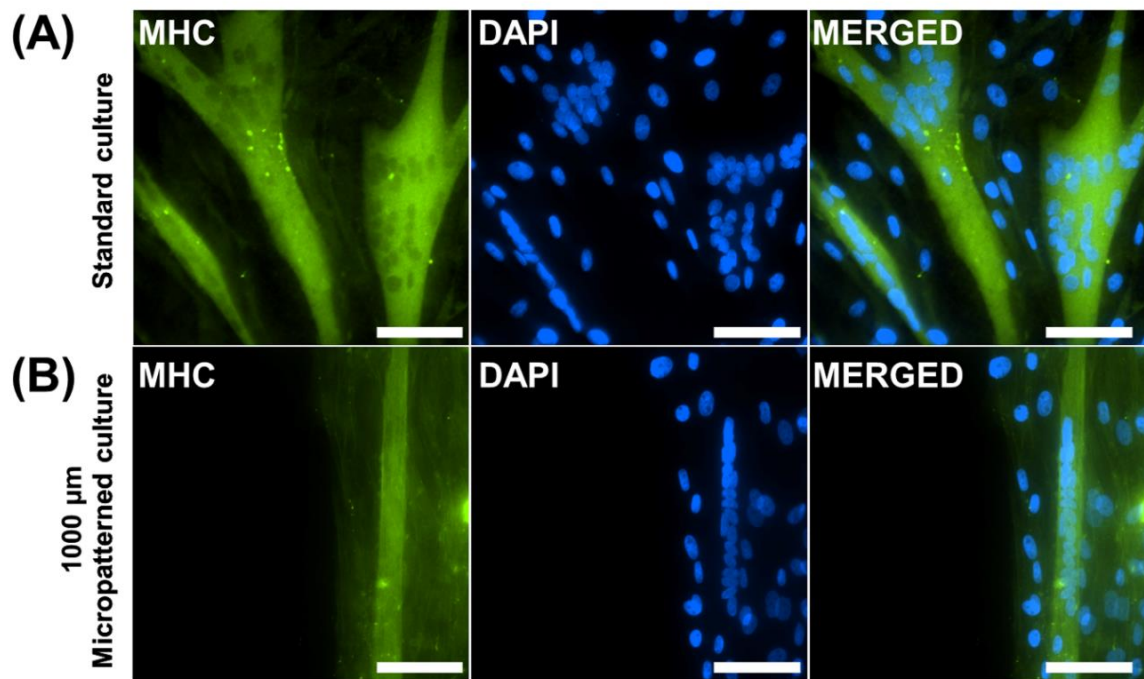
Figure 6.7 Characterization of myoblast differentiation on standard and micropatterned substrates. Fluorescent images of cells stained with anti-MHC (MHC, green) antibody and DAPI (nuclei, blue) of (A) standard Petri plate and (B) micropatterned (1000 µm) cultures after 14 days of in vitro culture (Scale bar: 50 µm).
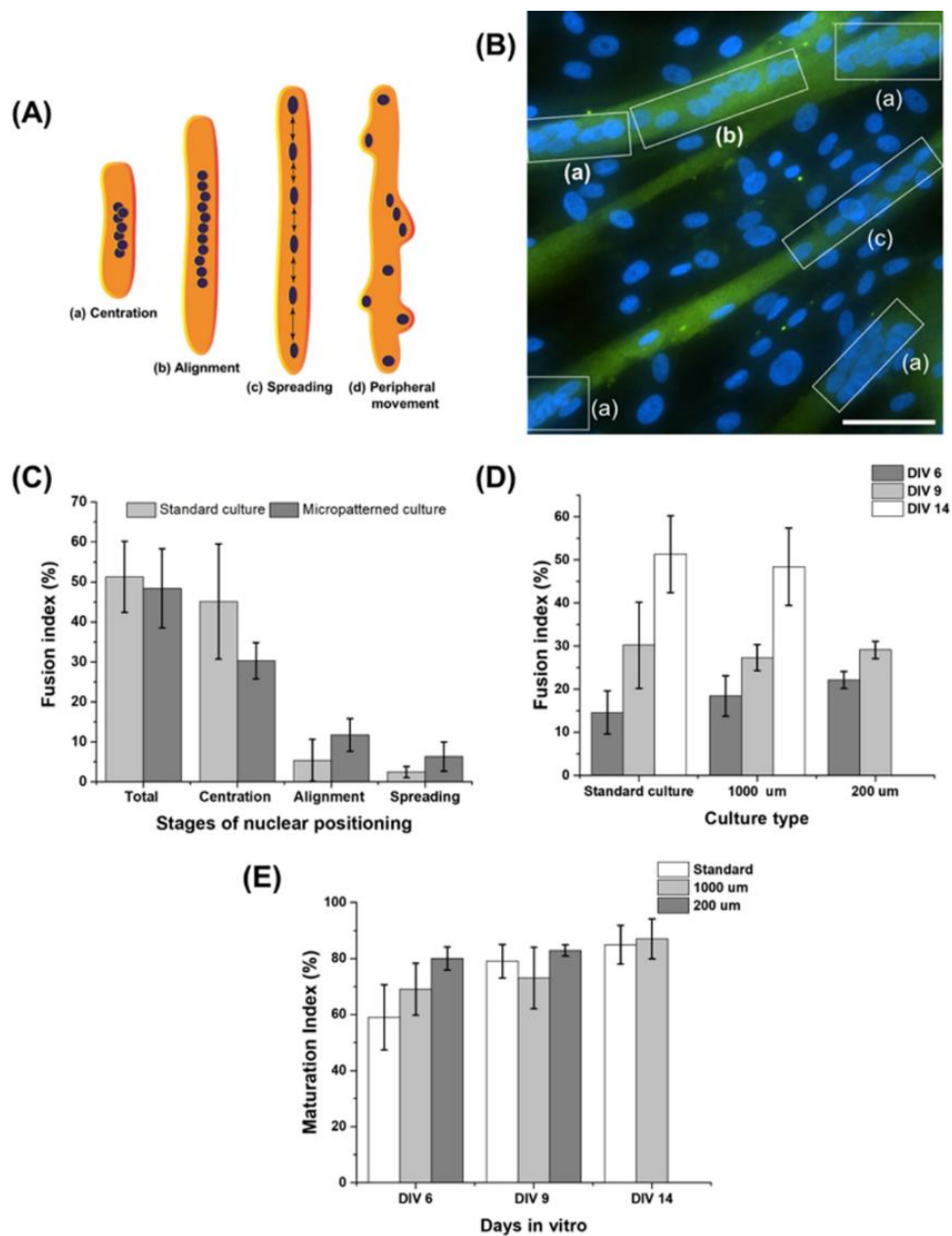
Figure 6.8 (A) Schematic of the stages of nuclear positioning present within a developing muscle cell. (B) Fluorescent image of myotubes stained with myosin heavy chain antibody (MHC, green) and DAPI (nuclei, blue) after 14 days in vitro culture, the insets (a) centration, (b) alignment and (c) spreading represent three different stages of nuclear positioning (Scale bar: 50 µm). (C) Results of the proposed fusion index method based on nuclear positioning for quantifying differentiation in standard Petri plate and micropatterned (1000 µm) cultures after 14 DIV. (D) Results of fusion index for quantifying differentiation in various culture types including standard, 1000 µm, and 200 µm. (E) Maturation index for quantifying differentiation after 14 days in culture. No significant differences were observed amongst the various fusion and maturation indices between standard and micropatterned culture conditions.

The images in the upperpanel (Figure 6.7A) illustrate the differentiation potential of the cells as the elongated structures, i.e., multinucleated myotubes are prominently seen although their patterns are quite irregular unlike the muscle fibres in vivo. Likewise, the image in the lower panel (Figure 6.7B) clearly depicts the formation of elongated myotubes in an aligned pattern, i.e., parallel to the interface of hydrophilic and hydrophobic regions. The appearance of such a well-defined arrangement of myotube on the micropatterned surface indicates the significant involvement of interplay between cell cues and surface topography which influences the differentiation of myotubes via myogenic regulatory factors (Bajaj et al., 2011)

The organisation of nuclei during myogenesis is one of the primary concerns during the process, as an improper arrangement of nuclei within the myotube may relate to musculopathological conditions (Dauer and Worman 2009; Metzger et al. 2012)**.** Nuclear organization in the myotubes cultured in vitro is reported to be subdivided into four steps including centration, alignment, spreading, and peripheral movement (Figure 6.8A, B). Centration involves microtubule and dynein-driven relocation of the newly fused cells' nucleus towards the centre of the myotube. In the alignment step, the nuclei line up along the major axis of the new myotube. Spreading is the process of even distribution of nuclei along the length of the myotube. Subsequently, peripheral migration of the nuclei takes place due myofibrillar rearrangement triggered contractility. Final step comprises securing of the nuclei at the periphery (W. Roman and Gomes 2018). Based on these stages of nuclei present in the elongated myotubes, an attempt was made to evaluate the fusion index, i.e., the number of nuclei involved in the formation of mature myotubes, and further enlist them in terms of centration, alignment and spreading fusion indices as shown in Figure 6.8B. Figure 6.8C represents the fusion index of nuclei within the myotubes observed in standard and micropatterned (1000 µm) cultures after 14 DIV.

Total fusion index in the standard culture conditions was estimated to be about 51% including centration, alignment, and spreading stages. Similarly, the total fusion index of the nuclei observed in micropatterned cultures was found to be 48%; thus, indicating no significant difference between both the cultures. In order to understand whether micropattering affects myotube fusion, the temporal variation of fusion index with respect to standard and different micropatterning widths (1000 µm and 200 µm) was carried out and is represented in Figure 6.8D. The figure shows variation of fusion index in standard and micropatterned widths for DIV 6, DIV 9 and DIV 14. The fusion index values were found to be showing no significant difference in their mean values at each of the days in vitro. Such observation of no significant difference in fusion index among linear micropatterns has been reported by Bajaj et.al. Further, the study had reported a significant decrease in fusion index of linear micropatterns with respect to standard conditions (Bajaj et al. 2011). Nevertheless, a direct analogy between the studies is difficult as the nature of substrates used i.e polystyrene plate (Bajaj et al.) and glass substrate (current study) is very different. Also, the cells used in the current case are primary statellite cells whereas C2C12 cells were studied by Bajaj et al. It was found that, at DIV 14 there was no significant difference between standard and 1000 µm patterned cultures. However, a significant increase in fusion index values were observed for standard, 1000 µm and 200 µm culture types over the period of in vitro culture (Figure 6.8D).

Maturation index was also used to determine the extent of differentiation among the standard and micropatterned cultures. Figure 6.8E represents the variation in maturation index of standard culture, 1000 µm and 200 µm patterns over the period of in vitro culture. Maturation index values for standard and 1000 µm patterned cultures were found to be 85% and 87% respectively at 14 DIV. As such, no significant difference is observed in

the maturation indices of all the culture conditions. The data from both maturation and fusion indices suggest that the isolated myoblasts were able to fuse and form multinucleated differentiated myotubes in both standard Petri plate and micropatterned cultures. The extent of differentiation in both the category of cultures were found to be similar. The reason for such an observation could be attributed to the wide-sized track used for micropatterning of the hydrophilic region (i.e., 1000 µm) that might have essentially behaved similarly to a standard petri plate. However, the influence of micropatterning on the alignment of myotubes was clearly noticeable through the morphological (Figure 6.5A) and MHC-stained fluorescence images (Figure 6.7B). The merit of dividing the fusion index data in terms of nuclear stages is of significance as the fusion index estimated by nuclear positioning provides an insight into the myogenesis of satellite cells; that otherwise may not be addressed when a total fusion index is simply considered.

6.3.5. Myotube width and distribution of nuclei across the width of myotubes

Another 2D morphometric characterization of the cells undergoing myogenesis includes the width of myotubes that has been typically used for estimating the size of myotubes (Fakhfakh, Michaud, and Tremblay 2011; Jacquemin et al. 2004; Rommel et al. 2001; Garcia et al. 2011)**.** Quantification of the size of myotubes found in standard and micropatterned (1000 µm) 14 DIV cultures resulted in an average diameter of about 21 µm and 13 µm, respectively, as shown in Figure 6.9A. To understand how the distribution of nuclei varies concerning the myotube diameter, the number of nuclei at various cross-sections of the myotubes was determined from the captured images. In DIV 14 standard culture, it was found that the number of nuclei varied across the myotube diameter from a minimum of one to a maximum of six (Figure 6.9B). The diameter of the myotube varied from a minimum of 8 µm incorporating one nucleus to a maximum of 54 µm

incorporating six nuclei. However, in the case of DIV 14 micropatterned culture of the cells, it was observed that the number of nuclei notably varied from a minimum of one to a maximum of two. Indeed, the myotube diameters encompassing the nuclei varied between a minimum of 6 µm incorporating one nucleus to a maximum of 20 µm incorporating two nuclei (Figure 6.9C).

The outcomes indicate that in standard culture the average myotube diameter and the number of nuclei incorporated along the myotube diameter are most likely due to a greater degree of fusion between myoblast–premyotube and premyotube-premyotube; that has been reported evidently in vivo by various studies (Harris et al. 1989; M. Zhang and McLennan 1995). In contrast, a significantly lower average myotube diameter and number of nuclei incorporated along the myotube diameter was observed in the case of micropatterned culture; that may be attributed to fusion influenced by the micropatterned environment. A study carried out by Clark *et al.* reported that culture of myoblasts on micropatterned laminin of varying widths resulted in the formation of myotubes of uniform diameter contrary to the expectation of a wider diameter of the myotubes (Clark, Coles, and Peckham 1997). Overall, the results obtained in both cases favour the fact that the distribution of nuclei within the myotubes depends on the cross-sectional areas of the myotubes that are determined by considering the diameter of myotubes (Bruusgaard et al. 2003).
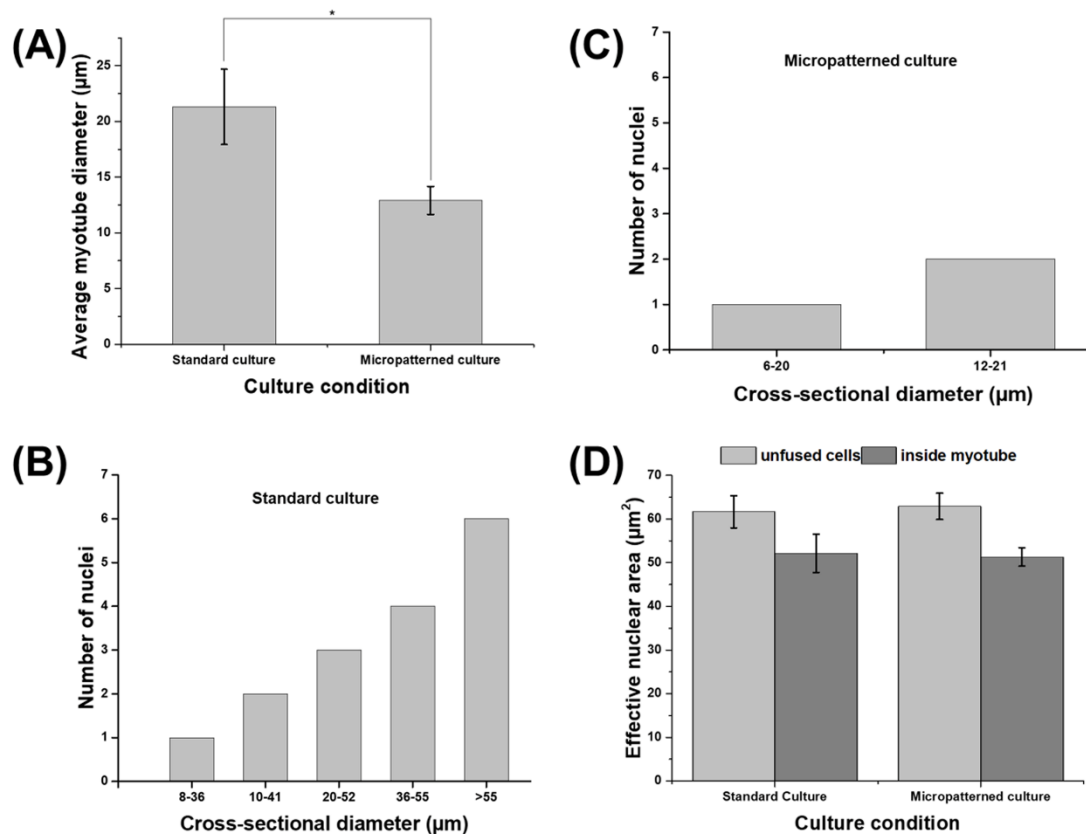
Figure 6.9 Morphometric characterisation of the cells undergoing myogenesis in standard and micropatterned (1000 µm) culture conditions (A) Average myotube diameter after 14 days in culture, *$p<0.05$ level of significance. (B) The variation in the number of nuclei with respect to their myotube diameters in standard culture conditions after 14 days. (C) Variation in the number of nuclei with respect to myotube diameters in micropatterned culture conditions after 14 days. (D) The effective area of the nuclei involved in myotubes and unfused cells of the cultures after 14 DIV.

### 6.3.6. Effective area of the nuclei present inside the myotube and unfused cells

Yet another way to quantify the fusion dynamics of the nuclear population is to determine the effective nuclear area inside the myotube and compare it with that of nuclei of the unfused cells. Figure 6.9D shows the plot for effective nuclear areas of the myotubes and unfused cells cultured in Petri plates and micropatterned (1000 µm) glass substrates after 14 DIV. The effective area of nuclei inside the myotube observed in standard culture conditions was found to be 52 µm^2. Whereas, the effective nuclear area of the unfused cells cultured in standard culture conditions was observed to be 62 µm^2 of the micropatterned substrate. Similarly, in the micropatterned culture the effective nuclear

area inside the myotubes was found to be 51 μm^2 while the same in unfused cells was observed to be 63 μm^2. No significant difference in the effective nuclear area inside the myotubes between standard Petri plate and micropatterned culture was observed. This observation is in coherence with the maturation index and fusion index, leading to the conclusion that the fusion events of the satellite cells within both the environments remained similar.

6.3.7. Determination of twitch frequency of spontaneous contractions in myotubes

One of the characteristics of functional skeletal muscle is contractility. Many groups have previously reported observations of spontaneous contractions by the myotubes in culture (Boonen et al. 2009; Dutton, Simon, and Burden 1993; J. M. Krebs and Denney 1997). Thus, it was necessary to characterise the level of twitch frequency exhibited by the myotubes spontaneously. A kymograph-based approach was followed for this examination (Bajaj et al., 2011)**.** Kymograph based approach is one of the non-invasive methods for quantifying contractile behaviour of myotubes using video data (Langhammer, Zahn, and Firestein, 2010). The outcomes of the kymograph-based examination (Figure 6.10A, B) reveals the twitch frequency of myotubes contracting spontaneously in both culture conditions. Plots to demonstrate variation in the amplitude of twitches with respect to time that is obtained from kymographs, as shown in Figure 6.10A(i) and 6.10B(i). Figure 6.10A(ii) and 6.10B(ii) represents a plot showing the power (which shows the strength of twitch signals) with regard to the frequency that is acquired by the FFT analysis of the graph illustrating amplitude versus time in the first column. Figure 6.10A(iii) and 6.10B(iii) represent the time series of images for myotube contraction under standard and micropatterned (1000 μm) condition, respectively.
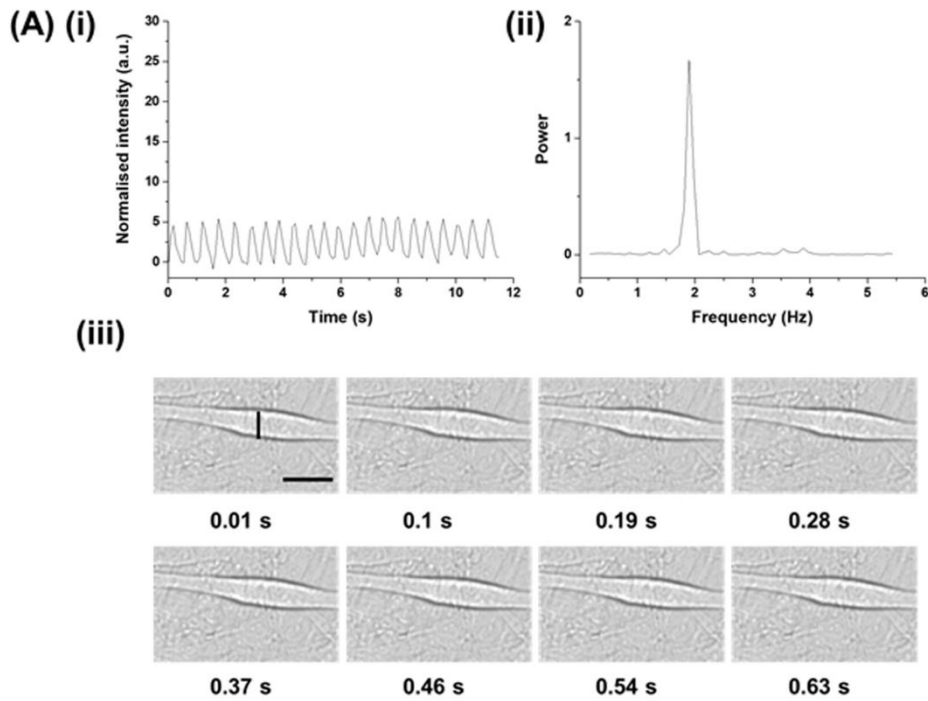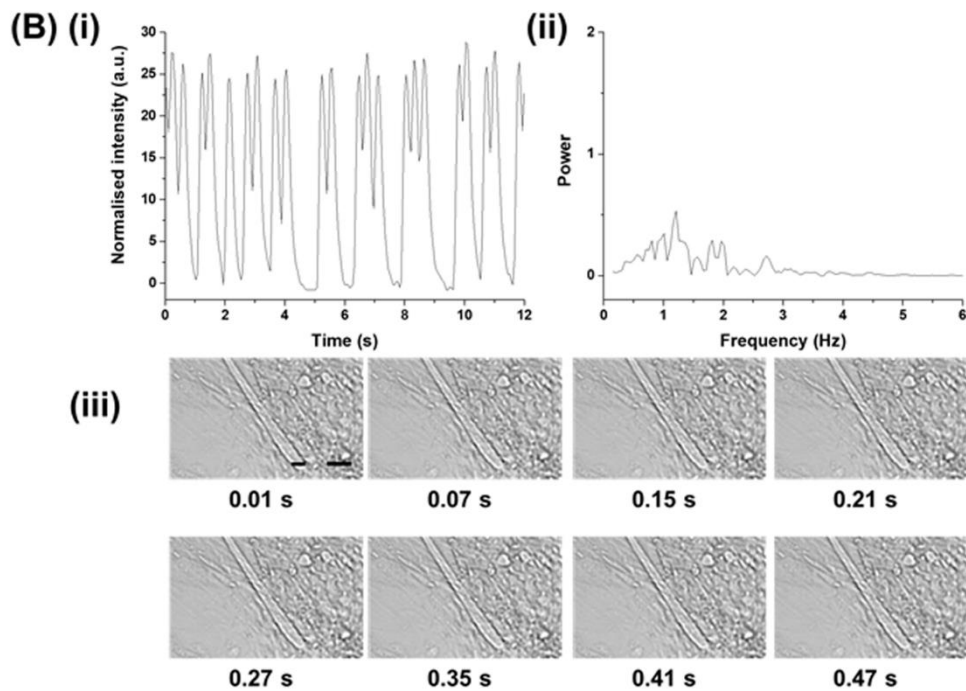
Figure 6.10 Functional characterisation of myotubes in standard and micropatterned (1000 μm) culture conditions (A) Analysis of twitch frequency for a myotube in standard culture (i) plot to demonstrate the variation in amplitude with respect to time (ii) plot showing the power of twitch signals with regard to frequency (iii) Time series images for myotube twitching under standard conditions showing line region of interest marked within the first image (Scale: 10 μm). (B) Analysis of twitch frequency for a myotube in

micropatterned culture (i) plot to demonstrate the variation in amplitude with respect to time (ii) plot showing the power of twitch signals with regard to frequency (iii) Time series images for myotube twitching under micropatterned conditions showing line region of interest marked within the first image (Scale: 10 µm).

Minute morphological movements are observed in the time series of images for myotube contraction. In Figure 6.10A(i) and 6.10B(i), the myotubes on micropatterned surface displayed an increased twitch amplitude compared to standard culture. Support for such observation could be found in various reports. Alignment of primary skeletal myoblasts by micropatterning leads to an increase in contractile force generation in engineered skeletal muscle tissues (Bian et al. 2011; Lam et al. 2009). In addition, studies performed in vascular smooth muscles and cardiac muscles indicate the noted role of a micropatterning technique for cellular alignment as well as for increased contractile behavior (Alford et al. 2011; Badie and Bursac 2009). The cells isolated from fast twitch muscles are known to retain the prominent expression of myosin isoforms MHC IIa and MHC IIb (Drzymala-Celichowska et al., 2012). These isoforms notably govern the contractile behaviour of the skeletal muscles. Thus, it could be anticipated that, the control of cells through micropatterning may increase the expression of the above MHC isoforms and result in enhanced contractility. In the plot, the frequency corresponding to the highest power peak represents the level of twitch frequency that was found to be 1.89 Hz and 1.21 Hz for the myotubes observed in standard and micropatterned cultures, respectively. A twitch frequency of 2 Hz and 0.3 Hz have been reported in the case of micropatterned primary skeletal myoblasts and cardiac muscle cells in a study by Cimetta et al. A slight increase in the frequency of twitch in primary skeletal myotubes compared to the case could be due to the usage of the hydrogel substrate with original tissue like stiffness (Cimetta et al. 2009). The myotubes observed on micropatterned surfaces showed a non-homogenous frequency compared to the standard culture conditions. Such variation in the

frequency could be attributed to a significant level of gradients of cell cues arising due to force anisotropy across the cell adhesive width. The outcomes indicate that the satellite origin cells differentiated and fused to form myotubes with functional sarcomere units that help in generation of spontaneous twitch forces.

6.3.8. Analysis of myotube alignment using Two-Dimensional Fast Fourier Transform (2D FFT)

Organized alignment of the muscle fibres is one of the most important characteristics required for full functionality of the skeletal muscle. In order to quantify the alignment of myotubes formed, immunofluorescence staining of myosin heavy chain was performed, and images were captured at 10X magnification. To determine the extent of alignment of the myotubes, the images were characterised by using 2D FFT (Ayres et al. 2006; Bajaj et al. 2011; 2014; N. F. Huang, Lee, and Li 2010). Figure 6.11 shows the FFT based alignment intensity vs angle in degree for both cases, i.e., standard (Figure 6.11A) and micropatterned (1000 µm) cultures (Figure 6.11B) at 14 DIV. The first column of each row represents the 14 DIV fluorescence images used for the 2D FFT analysis. The second column includes the 2D FFT obtained after the analysis of fluorescence images, and finally, the third row represents the plot of FFT alignment intensity vs angle in degree. The plot shows a representative principal angle of myotubes in a 360° space corresponding to the image. The level of myotube alignment is determined by comparing the height and shape of the peaks obtained (Ayres et al., 2006; Bajaj et al., 2011; Huang et al., 2010). In Figure 6.11A, it is observed that the number of peaks is estimated to be more than one, indicating the presence of random swirling patterns of myotubes in standard Petri plate culture as is visible from the corresponding immunofluorescence image. Whereas, in micropatterned (1000 µm) culture, a well-defined singular peak is observed as can be seen from the corresponding fluorescence images (Figure 6.11B). Such a single peak represents a high degree of myotube alignment along the angles

represented in the radial summation plot. In total, it was found that the isolated satellite cells in the absence of interplay of cell and surface cues formed randomly oriented myotubes (standard culture) whereas the presence of surface cues (1000 µm patterned substrates) lead to an aligned form of myotubes. 2D FFT analysis of myotubes allowed for an overall understanding of alignment of myotubes formed by the fusion of myoblasts in standard as well as micropatterned culture environments. This observation sheds light on the fact that the width of the micropatterned region is one of the important parameters when the alignment of cells is the primary area of concern. As observed, the larger surface area was available as the hydrophilic region for cell adhesion (i.e., 1000 µm width) in comparison to narrower cell adhesive regions ranging from 10 µm-500 µm in other studies (Bajaj et al. 2011; N. F. Huang, Lee, and Li 2010; Zatti et al. 2012).
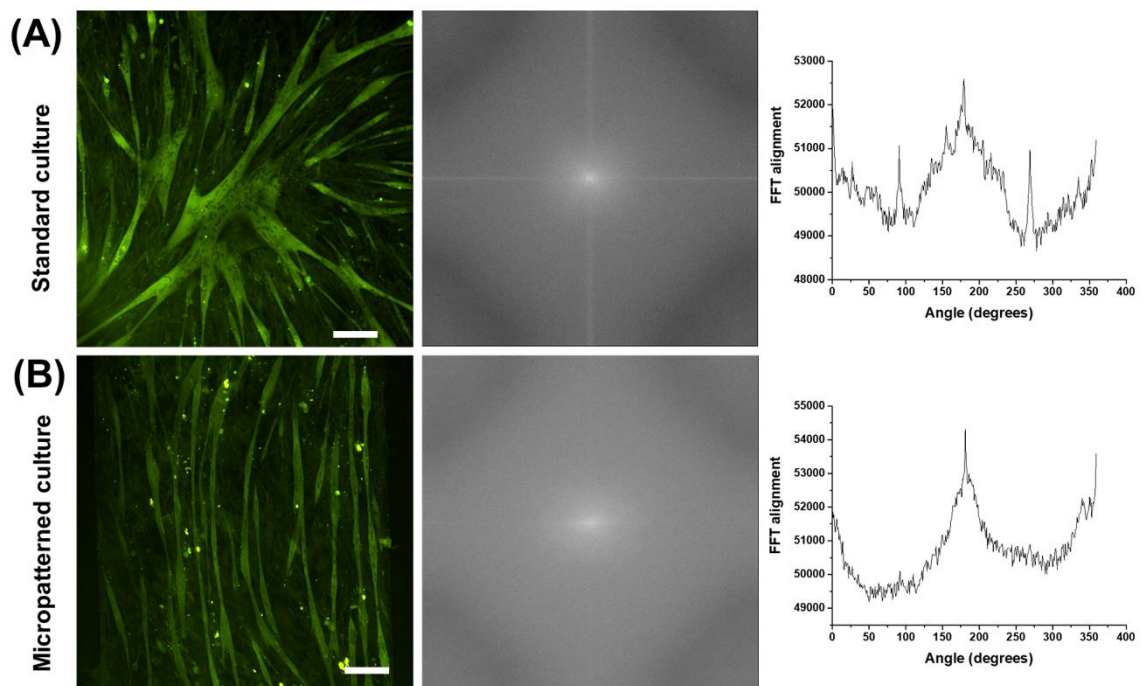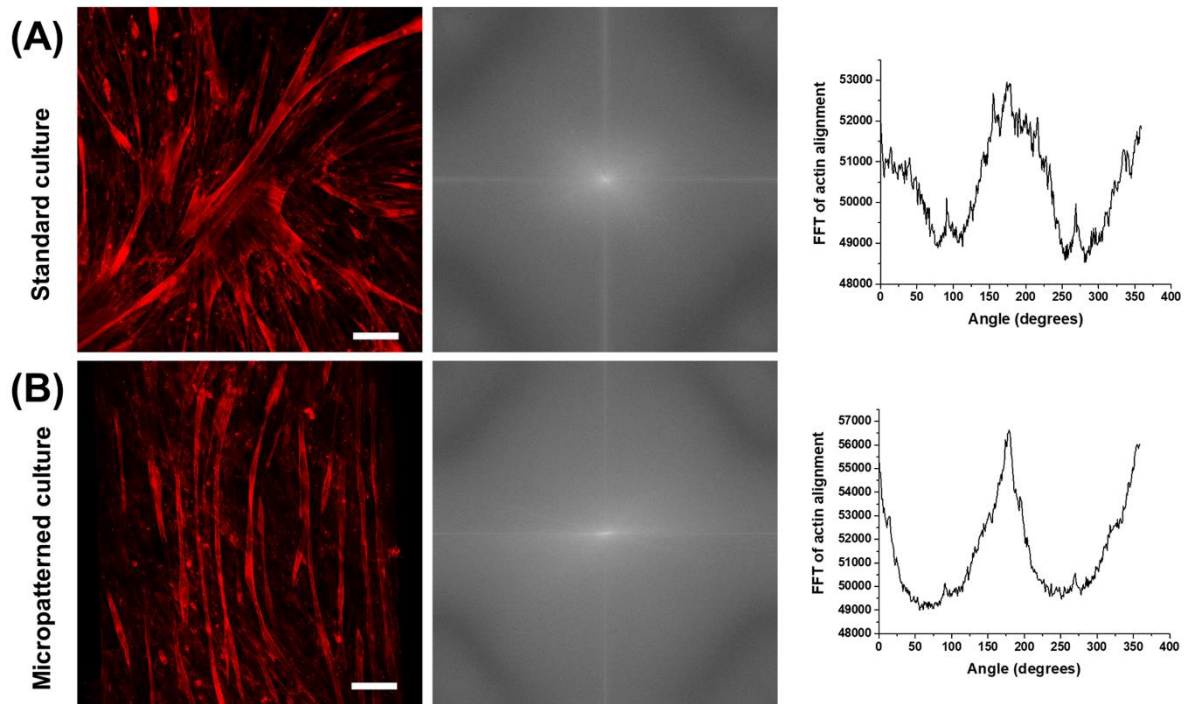

Figure 6.11 Analysis of myotube alignment using two-dimensional fast Fourier transform (A) Analysis of myotube alignment for fluorescence images stained with myosin heavy chain (green) obtained from standard culture (Scale bar: 100 µm). (B) Analysis of myotube alignment for fluorescence images stained with myosin heavy chain (green) obtained from micropatterned culture (Scale bar: 100 µm).

6.3.9. Analysis of myotube alignment using Two-Dimensional Fast Fourier Transform (2D FFT) using Actin Cytoskeleton

During in vitro fusion of myoblasts, the cells organize their actin and myosin 2A filaments to form the characteristic bipolar shape. Such bipolar shaped cells organize to form aligned groups. These bipolar shaped cells undergo fusion and form multinucleated myotubes (Peckham 2008). Myotubes undergo maturation to show contractility due to myosin and actin proteins. Therefore, 2D FFT based technique was employed to understand the extent of alignment in actin filaments in correlation to MHC stained myotubes. The 2D FFT alignment of the actin cytoskeleton was performed similarly to as described in Figure 6.11 except that the corresponding images stained for actin were processed. In Figure 6.12A the (right panel) image represents the fluorescent image stained for actin from standard Petri plate culture environment (14 DIV) corresponding to the region as shown in Figure 6.11A stained for myosin heavy chain. Further, the middle panel is the FFT output of the image. The third panel to the left represents the plot representing the FFT alignment of the actin cytoskeleton. Similarly, the fluorescent image of actin-stained region from micropatterned (1000 μm) culture (14 DIV) and its corresponding FFT plots along with the FFT of actin alignment plot have been represented in the right, middle and left panels of Figure 6.12B, corresponding to the region as shown in Figure 6.11B. It can be seen that the alignment plot for actin from standard culture conditions follows a similar trend as in the case of myotube alignment. An appearance of multiple numbers of peaks can be observed by moving move from 0° to 360°; thus, indicating no single alignment angle for actin cytoskeleton which is evident from the swirling pattern of myotubes observed in the fluorescent stained image for actin. In Figure 6.12B, the FFT of actin alignment in case of micropatterned culture shows a singular peak high-intensity peak at around 180°, suggesting that under the

150

micropatterned condition the actin cytoskeleton got majorly aligned under the influence of OTS/APTES induced micropatterned environment.

Figure 6.12 Analysis of actin cytoskeleton alignment using two-dimensional fast Fourier transform (A) Analysis of actin alignment for fluorescence images stained with rhodaminephalloidin (red) in relation to myotubes in Figure 6.11 (A) obtained from standard culture (Scale bar: 100 µm). (E) Analysis of actin alignment for fluorescence images stained with rhodaminephalloidin (red) in relation to myotubes in Figure 6.11 (B) obtained from micropatterned culture (Scale bar: 100 µm).

The results show a trend of alignment of actin cytoskeleton similar to those of the myotube alignment wherein standard culture conditions with no cues lead to a random alignment of actin and a single uniform peak for their alignment in case of the micropatterned surface. The results obtained from the FFT analysis of cytoskeletal MHC and actin are in accordance with the OOP results indicating the overall improvement in alignment of myoblasts under the micropatterned condition.

In this chapter, the microchannel flowed plasma process used in chapter 5 for understanding alignment of C2C12 cells was used. The micropatterning technique is used for the first time to study the influence of substrate patterning on primary satellite cells

isolated from rat hind limb muscles. The use of primary skeletal muscle cells is justified as they show greater physiological relevance compared to C2C12 cells. While various micropatterning studies have been carried out to study C2C12 cells (Yamamoto et al. 2008; Gingras et al. 2009; N. F. Huang, Lee, and Li 2010; Bajaj et al. 2011; Zatti et al. 2012). There is a scarcity of micropatterning studies utilising primary skeletal muscle cells from mice (Cimetta et al. 2009) and primary human skeletal muscle cell (Duffy, Sun, and Feinberg 2016; Zatti et al. 2012). While the use of 1000 µm micropattern was applied by Junkin et al. to show the long-distance self-organization behaviour of C2C12 myoblasts to form organized structure of skeletal muscle (Junkin, Leung, Whitman, et al. 2011). The current study attempted to study the long-distance alignment of primary rat skeletal muscle cells over microchannel flowed plasma processed 1000 µm pattern for a period of 14 days and in addition to it characterization of aligned myotubes with respect to their fusion index, maturation index, average width of the myotubes and characterization of spontaneous twitch frequency was carried out.

6.4. Summary

To summarize, in order to study the influence of micropatterning on myogenesis, primary myoblasts were characterised and cultured on micropatterned and standard Petriplate substrates. The myoblasts cultured in standard Petri plates and micropatterned conditions for 14 days differentiated and fused to exhibit the characteristic myosin heavy chain prominently. Further, morphometric based image analytical methods were established to explore the sequential events of myogenesis process in vitro. Myotubes were analysed for estimating the fusion index considering the different stages of nuclear positioning during myogenesis; that provides comprehensive information regarding the extent and progression of differentiation in myoblasts in vitro. 2D FFT based examination and OOP analysis revealed the overall orientation of the myotubes in the variable culture

conditions. Myotubes in micropatterned culture were noticeably better aligned to each other compared to those of culture plates due to contact guidance-based mechanism of cell-cell communication. Similar observations were obtained for their respective actin cytoskeleton. Based on the observations, myotubes exhibiting increased twitch amplitude under micropatterned conditions compared to standard culture conditions indicated that micropatterned culture might lead to the formation of relatively mature myotubes. These observations lay the groundwork for the future work focused on influence of micropatterning on contractility of myotubes. Overall, results suggest that the contact guidance cues arising due to micropatterning of the substrates could be a key regulator for controlling the size and degree of alignment of myotubes during the myogenesis process.